

Bosonic decays of \tilde{t}_2 and \tilde{b}_2

A. Bartl^a, H. Eberl^b, K. Hidaka^c, S. Kraml^b, T. Kon^d,
W. Majerotto^b, W. Porod^a, and Y. Yamada^e

^a*Institut für Theoretische Physik, Universität Wien, A-1090 Vienna, Austria*

^b*Institut für Hochenergiephysik der Österreichischen Akademie der Wissenschaften,
A-1050 Vienna, Austria*

^c*Department of Physics, Tokyo Gakugei University, Koganei, Tokyo 184-8501, Japan*

^d*Faculty of Engineering, Seikei University, Musashino, Tokyo 180, Japan*

^e*Department of Physics, Tohoku University, Sendai 980-8578, Japan*

Abstract

We perform a detailed study of the decays of the heavier top and bottom squarks (\tilde{t}_2 and \tilde{b}_2) in the Minimal Supersymmetric Standard Model (MSSM). We show that the decays into Higgs or gauge bosons, i.e. $\tilde{t}_2 \rightarrow \tilde{t}_1 + (h^0, H^0, A^0 \text{ or } Z^0)$, $\tilde{t}_2 \rightarrow \tilde{b}_{1,2} + (H^+ \text{ or } W^+)$, and the analogous \tilde{b}_2 decays, can be dominant in a wide range of the model parameters due to the large Yukawa couplings and mixings of \tilde{t} and \tilde{b} . Compared to the conventional decays into fermions, such as $\tilde{t}_2 \rightarrow t + (\tilde{\chi}_i^0 \text{ or } \tilde{g})$ and $\tilde{t}_2 \rightarrow b + \tilde{\chi}_j^+$, these bosonic decay modes can have significantly different decay structures and distributions. This could have an important impact on the search for \tilde{t}_2 and \tilde{b}_2 and the determination of the MSSM parameters at future colliders.

The search for supersymmetric (SUSY) particles is one of the most important subjects at present and future collider experiments. Future colliders, such as the Large Hadron Collider (LHC), the upgraded Tevatron, e^+e^- linear colliders, and $\mu^+\mu^-$ colliders will extend the discovery potential for SUSY particles to the TeV mass range and allow for a precise determination of the SUSY parameters.

Many phenomenological and experimental studies have been performed for squark (\tilde{q}) search [1]. In most studies, production and decay of the squarks are studied assuming that they decay into fermions, i. e. a quark plus a neutralino ($\tilde{\chi}_k^0$), chargino ($\tilde{\chi}_j^\pm$), or gluino (\tilde{g}):

$$\tilde{q}_i \rightarrow q^{(\prime)} + (\tilde{\chi}_k^0, \tilde{\chi}_j^\pm, \text{ or } \tilde{g}), \quad (1)$$

with $i, j = 1, 2$ and $k = 1, \dots, 4$. However, in the Minimal Supersymmetric Standard Model (MSSM) [2] the heavier squarks of the 3rd generation (i.e. stops (\tilde{t}_2) and sbottoms (\tilde{b}_2)) can also decay into bosons, i. e. a lighter squark plus a gauge or Higgs boson [3, 4]:

$$\begin{aligned} \tilde{t}_2 &\rightarrow \tilde{t}_1 Z^0, & \tilde{b}_2 &\rightarrow \tilde{b}_1 Z^0, \\ \tilde{t}_2 &\rightarrow \tilde{b}_i W^+, & \tilde{b}_2 &\rightarrow \tilde{t}_i W^-, \end{aligned} \quad (2)$$

and

$$\begin{aligned} \tilde{t}_2 &\rightarrow \tilde{t}_1 (h^0, H^0, A^0), & \tilde{b}_2 &\rightarrow \tilde{b}_1 (h^0, H^0, A^0), \\ \tilde{t}_2 &\rightarrow \tilde{b}_i H^+, & \tilde{b}_2 &\rightarrow \tilde{t}_i H^-. \end{aligned} \quad (3)$$

Here \tilde{q}_1 (\tilde{q}_2) is the lighter (heavier) squark mass eigenstate. The \tilde{t}_2 decays into \tilde{t}_1 plus a neutral boson in Eqs. (2) and (3) are possible in case the difference between $m_{\tilde{t}_L}$ and $m_{\tilde{t}_R}$ and/or the \tilde{t}_L - \tilde{t}_R mixing are large enough to make the necessary mass splitting between \tilde{t}_1 and \tilde{t}_2 . The same holds for the decays $\tilde{b}_2 \rightarrow \tilde{b}_1 + (Z^0, h^0, H^0, A^0)$.

In the present article we make a more general analysis than [3, 4]. We point out that the \tilde{q}_2 decays into gauge or Higgs bosons of Eqs. (2) and (3) can be dominant in a large region of the MSSM parameter space due to large top and bottom Yukawa couplings and large \tilde{t} and \tilde{b} mixing parameters. This dominance of the Higgs/gauge boson modes over the conventional fermionic modes of Eq. (1) could have a crucial impact on searches for \tilde{t}_2 and \tilde{b}_2 at future colliders.

First we summarize the MSSM parameters in our analysis. In the MSSM the squark sector is specified by the squark mass matrix in the basis $(\tilde{q}_L, \tilde{q}_R)$ with $\tilde{q} = \tilde{t}$ or \tilde{b} [5, 6]

$$\mathcal{M}_{\tilde{q}}^2 = \begin{pmatrix} m_{\tilde{q}_L}^2 & a_q m_q \\ a_q m_q & m_{\tilde{q}_R}^2 \end{pmatrix} \quad (4)$$

with

$$m_{\tilde{q}_L}^2 = M_{\tilde{Q}}^2 + m_Z^2 \cos 2\beta (I_{3L}^q - e_q \sin^2 \theta_W) + m_q^2, \quad (5)$$

$$m_{\tilde{q}_R}^2 = M_{\{\tilde{U}, \tilde{D}\}}^2 + m_Z^2 \cos 2\beta e_q \sin^2 \theta_W + m_q^2, \quad (6)$$

$$a_q m_q = \begin{cases} (A_t - \mu \cot \beta) m_t & (\tilde{q} = \tilde{t}) \\ (A_b - \mu \tan \beta) m_b & (\tilde{q} = \tilde{b}). \end{cases} \quad (7)$$

Here I_3^q is the third component of the weak isospin and e_q the electric charge of the quark q . $M_{\tilde{Q}, \tilde{U}, \tilde{D}}$ and $A_{t,b}$ are soft SUSY-breaking parameters, μ is the higgsino mass parameter, and $\tan \beta = v_2/v_1$ with v_1 (v_2) being the vacuum expectation value of the Higgs H_1^0 (H_2^0). From renormalization group equations we expect that $M_{\tilde{Q}}$, $M_{\tilde{U}}$, and $M_{\tilde{D}}$ of the third generation are different from those of the first two generations and from each other. Diagonalizing the matrix (4) one gets the mass eigenstates $\tilde{q}_1 = \tilde{q}_L \cos \theta_{\tilde{q}} + \tilde{q}_R \sin \theta_{\tilde{q}}$, $\tilde{q}_2 = -\tilde{q}_L \sin \theta_{\tilde{q}} + \tilde{q}_R \cos \theta_{\tilde{q}}$ with the masses $m_{\tilde{q}_1}$, $m_{\tilde{q}_2}$ ($m_{\tilde{q}_1} < m_{\tilde{q}_2}$) and the mixing angle $\theta_{\tilde{q}}$. As can be seen, sizable mixing effects can be expected in the stop sector due to the large top quark mass. Likewise, \tilde{b}_L - \tilde{b}_R mixing may be important for large $\tan \beta$.

The properties of the charginos $\tilde{\chi}_i^\pm$ ($i = 1, 2$; $m_{\tilde{\chi}_1^\pm} < m_{\tilde{\chi}_2^\pm}$) and neutralinos $\tilde{\chi}_k^0$ ($k = 1, \dots, 4$; $m_{\tilde{\chi}_1^0} < \dots < m_{\tilde{\chi}_4^0}$) are determined by the parameters M , M' , μ and $\tan \beta$, where M and M' are the SU(2) and U(1) gaugino masses, respectively. Assuming gaugino mass unification we take $M' = (5/3) \tan^2 \theta_W M$ and $m_{\tilde{g}} = (\alpha_s(m_{\tilde{g}})/\alpha_2) M$ with $m_{\tilde{g}}$ being the gluino mass. The masses and couplings of the Higgs bosons h^0 , H^0 , A^0 and H^\pm , including leading Yukawa corrections, are fixed by m_A , $\tan \beta$, μ , m_t , m_b , $M_{\tilde{Q}}$, $M_{\tilde{U}}$, $M_{\tilde{D}}$, A_t , and A_b . H^0 (h^0) and A^0 are the heavier (lighter) CP-even and CP-odd neutral Higgs bosons, respectively. For the Yukawa corrections to the h^0 and H^0 masses and their mixing angle α we use the formulae of Ref. [7]. For H^\pm we take $m_{H^\pm}^2 = m_A^2 + m_W^2$.

The widths of the squark decays into Higgs and gauge bosons are given by ($i, j = 1, 2$; $k = 1 \dots 4$) [3]:

$$\Gamma(\tilde{q}_i \rightarrow \tilde{q}_j^{(\prime)} H_k) = \frac{\kappa_{ijk}}{16\pi m_{\tilde{q}_i}^3} (G_{ijk})^2, \quad \Gamma(\tilde{q}_i \rightarrow \tilde{q}_j^{(\prime)} V) = \frac{\kappa_{ijV}^3}{16\pi m_V^2 m_{\tilde{q}_i}^3} (c_{ijV})^2. \quad (8)$$

Here $H_k = \{h^0, H^0, A^0, H^\pm\}$ and $V = \{Z^0, W^\pm\}$. The G_{ijk} denote the squark couplings to Higgs bosons and c_{ijV} those to gauge bosons. $\kappa_{ijX} \equiv \kappa(m_{\tilde{q}_i}^2, m_{\tilde{q}_j^{(\prime)}}^2, m_X^2)$ is the usual kinematic factor, $\kappa(x, y, z) = (x^2 + y^2 + z^2 - 2xy - 2xz - 2yz)^{1/2}$. (Notice that $\Gamma(\tilde{q}_i \rightarrow \tilde{q}_j^{(\prime)} H_k)$ is proportional to κ whereas $\Gamma(\tilde{q}_i \rightarrow \tilde{q}_j^{(\prime)} V)$ is proportional to κ^3 .) The complete expressions for G_{ijk} and c_{ijV} , as well as the widths of the fermionic modes, are given in [3, 8]. The leading terms of the squark couplings to Higgs and vector bosons are given in Table 1. The Yukawa couplings $h_{t,b}$ are given as

$$h_t = g m_t / (\sqrt{2} m_W \sin \beta), \quad h_b = g m_b / (\sqrt{2} m_W \cos \beta). \quad (9)$$

As can be seen, the $\tilde{q}_1 \tilde{q}_2 Z^0$ couplings take their maximum for full \tilde{q}_L - \tilde{q}_R mixing ($\theta_{\tilde{q}} \rightarrow \pi/4$ or $3\pi/4$) and vanish in case of no mixing. The reason is that the Z^0 couples only to $\tilde{q}_L^\dagger \tilde{q}_L$ and $\tilde{q}_R^\dagger \tilde{q}_R$. On the other hand, the W^\pm couples only to the left components of the squarks. In contrast to that, Higgs bosons couple mainly to \tilde{q}_L - $\tilde{q}_R^{(\prime)}$ combinations. These couplings are proportional to the Yukawa couplings $h_{t,b}$ and the parameters $A_{t,b}$ and μ , as can be seen in Table 1. Notice here that the $\tilde{q}_1 \tilde{q}_2 h^0$ and $\tilde{q}_1 \tilde{q}_2 H^0$ couplings have a factor $\cos 2\theta_{\tilde{q}}$ (which decreases with increase of the \tilde{q} -mixing) while the $\tilde{q}_1 \tilde{q}_2 A^0$ couplings do not depend explicitly on the squark mixing angles. Hence the $\tilde{t}_1 \tilde{t}_2 A^0$ coupling (and the $\tilde{b}_1 \tilde{b}_2 A^0$ coupling for large $\tan \beta$) can be especially strong in case A_t (A_b) and μ are large. Notice

$$\begin{array}{lcl}
\tilde{t}_1 \tilde{t}_2 Z^0 & \sim & g \sin 2\theta_{\tilde{t}} \\
\tilde{t}_1 \tilde{t}_2 h^0 & \sim & h_t (\mu \sin \alpha + A_t \cos \alpha) \cos 2\theta_{\tilde{t}} \\
\tilde{t}_1 \tilde{t}_2 H^0 & \sim & h_t (\mu \cos \alpha - A_t \sin \alpha) \cos 2\theta_{\tilde{t}} \\
\tilde{t}_1 \tilde{t}_2 A^0 & \sim & h_t (\mu \sin \beta + A_t \cos \beta)
\end{array}
\left|
\begin{array}{lcl}
\tilde{b}_1 \tilde{b}_2 Z^0 & \sim & g \sin 2\theta_{\tilde{b}} \\
\tilde{b}_1 \tilde{b}_2 h^0 & \sim & h_b (\mu \cos \alpha + A_b \sin \alpha) \cos 2\theta_{\tilde{b}} \\
\tilde{b}_1 \tilde{b}_2 H^0 & \sim & h_b (\mu \sin \alpha - A_b \cos \alpha) \cos 2\theta_{\tilde{b}} \\
\tilde{b}_1 \tilde{b}_2 A^0 & \sim & h_b (\mu \cos \beta + A_b \sin \beta)
\end{array}
\right.$$

$$\begin{array}{lcl}
\tilde{t}_1 \tilde{b}_1 H^\pm & \sim & h_t (\mu \sin \beta + A_t \cos \beta) \sin \theta_{\tilde{t}} \cos \theta_{\tilde{b}} + h_b (\mu \cos \beta + A_b \sin \beta) \cos \theta_{\tilde{t}} \sin \theta_{\tilde{b}} \\
\tilde{t}_1 \tilde{b}_2 H^\pm & \sim & -h_t (\mu \sin \beta + A_t \cos \beta) \sin \theta_{\tilde{t}} \sin \theta_{\tilde{b}} + h_b (\mu \cos \beta + A_b \sin \beta) \cos \theta_{\tilde{t}} \cos \theta_{\tilde{b}} \\
\tilde{t}_2 \tilde{b}_1 H^\pm & \sim & h_t (\mu \sin \beta + A_t \cos \beta) \cos \theta_{\tilde{t}} \cos \theta_{\tilde{b}} - h_b (\mu \cos \beta + A_b \sin \beta) \sin \theta_{\tilde{t}} \sin \theta_{\tilde{b}} \\
\tilde{t}_2 \tilde{b}_2 H^\pm & \sim & -h_t (\mu \sin \beta + A_t \cos \beta) \cos \theta_{\tilde{t}} \sin \theta_{\tilde{b}} - h_b (\mu \cos \beta + A_b \sin \beta) \sin \theta_{\tilde{t}} \cos \theta_{\tilde{b}}
\end{array}$$

$$\tilde{t}_i \tilde{b}_j W^\pm \sim g \begin{pmatrix} \cos \theta_{\tilde{t}} \cos \theta_{\tilde{b}} & -\cos \theta_{\tilde{t}} \sin \theta_{\tilde{b}} \\ -\sin \theta_{\tilde{t}} \cos \theta_{\tilde{b}} & \sin \theta_{\tilde{t}} \sin \theta_{\tilde{b}} \end{pmatrix}_{ij}$$

Table 1: *Squark couplings to Higgs and vector bosons (leading terms).*

also that the squark mixing angles themselves depend on $A_{t,b}$, μ , and $\tan \beta$. Moreover, \tilde{q}_L - \tilde{q}_R mixing enhances the splitting of the \tilde{q} mass eigenvalues, which in turn can have an important influence on the phase space of the \tilde{q}_2 decays.

We now turn to the numerical analysis of the \tilde{t}_2 and \tilde{b}_2 decay branching ratios. For this, we calculate the widths of all possibly important 2-body decay modes (3-body decays [8] are negligible in this study):

$$\begin{array}{lcl}
\tilde{t}_2 & \rightarrow & t\tilde{g}, t\tilde{\chi}_k^0, b\tilde{\chi}_j^+, \tilde{t}_1 Z^0, \tilde{b}_1 W^+, \tilde{t}_1 h^0, \tilde{t}_1 H^0, \tilde{t}_1 A^0, \tilde{b}_1 H^+, \\
\tilde{b}_2 & \rightarrow & b\tilde{g}, b\tilde{\chi}_k^0, t\tilde{\chi}_j^-, \tilde{b}_1 Z^0, \tilde{t}_1 W^-, \tilde{b}_1 h^0, \tilde{b}_1 H^0, \tilde{b}_1 A^0, \tilde{t}_1 H^-.
\end{array}$$

We take $m_t = 175$ GeV, $m_b = 5$ GeV, $m_Z = 91.2$ GeV, $\sin^2 \theta_W = 0.23$, $m_W = m_Z \cos \theta_W$, $\alpha(m_Z) = 1/129$, and $\alpha_s(m_Z) = 0.12$ [with $\alpha_s(Q) = 12\pi/((33-2n_f) \ln(Q^2/\Lambda_{n_f}^2))$, n_f being the number of quark flavors]. In order not to vary many parameters we choose $M_{\tilde{Q}} = \frac{9}{8}M_{\tilde{U}} = \frac{9}{10}M_{\tilde{D}}$ and $A_t = A_b \equiv A$ for simplicity. Moreover, we fix $M = 300$ GeV (i.e. $m_{\tilde{g}} = 820$ GeV) and $m_A = 150$ GeV. Thus we have as free parameters $M_{\tilde{Q}}$, μ , $\tan \beta$, and A . In the plots we impose the following conditions:

- (i) $m_{\tilde{\chi}_1^\pm} > 100$ GeV,
- (ii) $m_{\tilde{\chi}_1^0} > 70$ GeV,
- (iii) $m_{\tilde{t}_1, \tilde{b}_1} > m_{\tilde{\chi}_1^0}$,
- (iv) $m_{h^0} > 80$ GeV,
- (v) $\Delta\rho(\tilde{t}-\tilde{b}) < 0.0016$ [9] using the formula of [10], and

- (vi) $A_t^2 < 3(M_{\tilde{Q}}^2 + M_{\tilde{U}}^2 + m_{H_2}^2)$ and $A_b^2 < 3(M_{\tilde{Q}}^2 + M_{\tilde{D}}^2 + m_{H_1}^2)$ with
 $m_{H_2}^2 = (m_A^2 + m_Z^2) \cos^2 \beta - \frac{1}{2} m_Z^2$ and $m_{H_1}^2 = (m_A^2 + m_Z^2) \sin^2 \beta - \frac{1}{2} m_Z^2$
(approximately necessary conditions to avoid colour and electric charge breaking
global minimum [11]).

Conditions (i)–(iv), along with $m_{\tilde{g}} = 820$ GeV, satisfy the experimental bounds on $\tilde{\chi}_1^+$, $\tilde{\chi}_1^0$, \tilde{t} , \tilde{b} , and h^0 from LEP2 [12, 13, 14] and Tevatron [15]. Conditions (v) and (vi) constrain the \tilde{t} and \tilde{b} mixings significantly.

In Fig. 1 we plot the contour lines for the branching ratios of the Higgs boson modes and the gauge boson modes, i. e. $\text{BR}(\tilde{q}_2 \rightarrow \tilde{q}^{(\prime)} H) \equiv \sum \text{BR}[\tilde{q}_2 \rightarrow \tilde{q}_1 + (h^0, H^0, A^0), \tilde{q}'_{1,2} + H^\pm]$ and $\text{BR}(\tilde{q}_2 \rightarrow \tilde{q}^{(\prime)} V) \equiv \sum \text{BR}[\tilde{q}_2 \rightarrow \tilde{q}_1 + Z^0, \tilde{q}'_{1,2} + W^\pm]$ with $\tilde{q} = \tilde{t}$ or \tilde{b} , in the μ – A plane for $M_{\tilde{Q}} = 500$ GeV and $\tan \beta = 3$. We see that the \tilde{t}_2 and \tilde{b}_2 decays into bosons are dominant in a large region of the MSSM parameter space, in particular for large $|\mu|$ and/or $|A|$. Note here the dependence on the signs of A and μ . We have obtained a similar result for large $\tan \beta$.

In Fig. 2 we show the individual branching ratios of the \tilde{t}_2 and \tilde{b}_2 decays into bosons as a function of μ for $M_{\tilde{Q}} = 500$ GeV, $A = 600$ GeV, (a) $\tan \beta = 3$ and (b, c) $\tan \beta = 30$. (We plot only branching ratios larger than 1%.) In case of $\tan \beta = 3$ (Fig. 2a) the bosonic decays of \tilde{t}_2 are dominant ($\text{BR} \gtrsim 50\%$) for $\mu \lesssim -400$ GeV because (i) $(A_t - \mu \cot \beta) m_t$, the off-diagonal element of the stop mass matrix, is large enough to induce the necessary mixing and mass splitting for the stops, and (ii) for relatively large $|\mu|$ the decays into higgsino-like neutralinos ($\tilde{\chi}_{3,4}^0$) and chargino ($\tilde{\chi}_2^\pm$) are kinematically suppressed or forbidden. The branching ratio of the $\tilde{t}_1 Z^0$ mode has its maximum at $\mu = -600$ GeV where $m_{\tilde{t}_1} = 332$ GeV, $m_{\tilde{t}_2} = 628$ GeV, and $\theta_{\tilde{t}} \simeq 130^\circ$. For further decreasing μ the decay into $\tilde{t}_1 A^0$ quickly gains importance as the $\tilde{t}_1 \tilde{t}_2 A^0$ coupling is $\sim h_t(0.3 A_t + 0.95 \mu)$. The $\tilde{b}_1 W^+$ mode has a branching ratio of 10% to 16% for $\mu \lesssim -400$ GeV because $\tilde{b}_1 \sim \tilde{b}_L$ and $m_{\tilde{b}_1} \simeq 500$ GeV. For positive μ the bosonic \tilde{t}_2 decays are kinematically suppressed or even forbidden due to insufficient stop mass splitting. Similar arguments hold for the \tilde{b}_2 decays. Here only the decays into $\tilde{t}_1 H^-$ and $\tilde{t}_1 W^-$ are kinematically accessible, which can be seen in Figs. 1c and 1d.

For $\tan \beta = 30$ (Figs. 2b and 2c) there is a large mixing also in the sbottom sector (which is proportional to $\mu \tan \beta$ while $\theta_{\tilde{t}} \sim 128^\circ$, see Eq. (7)). Hence the \tilde{t}_2 and \tilde{b}_2 decay branching ratios show a much weaker dependence on the sign of μ . For $|\mu| \gtrsim 400$ GeV the decays into bosons clearly dominate. Notice the importance of the decays $\tilde{t}_2 \rightarrow \tilde{b}_1 + (H^+, W^+)$ in Fig. 2b and $\tilde{b}_2 \rightarrow \tilde{b}_1 + (A^0, Z^0)$ in Fig. 2c. This is mainly due to the large mixing (and hence large mass splitting) in the sbottom sector. Notice also that, in general, when the decays into Z^0 and A^0 are kinematically allowed, those into h^0 and H^0 are also possible. The latter decays are, however, practically negligible in this example because they are suppressed by a factor $\cos^2 2\theta_{\tilde{q}}$. (Here note that $\text{BR}(\tilde{t}_2 \rightarrow \tilde{t}_1 h^0)$ and $\text{BR}(\tilde{t}_2 \rightarrow \tilde{t}_1 H^0)$ can be about $\sim 10\%$ for other values of the MSSM parameters; see e.g. Fig. 4.)

In Fig. 3 we show the $\tan\beta$ dependence of the bosonic \tilde{t}_2 and \tilde{b}_2 decay branching ratios for $M_{\tilde{Q}} = 500$ GeV, $A = 600$ GeV, and $\mu = -700$ GeV. Here it can be seen explicitly how the \tilde{q}_2 decays into the lighter sbottom \tilde{b}_1 plus a gauge or Higgs boson become important with increasing $\tan\beta$.

In Fig. 4 we show the $M_{\tilde{Q}}$ dependence of the branching ratios of the bosonic \tilde{t}_2 and \tilde{b}_2 decays for $A = 400$ GeV, $\mu = -1000$ GeV, and $\tan\beta = 3$. In this case we have $(m_{\tilde{\chi}_1^0}, m_{\tilde{\chi}_1^+}, m_{\tilde{g}}) = (150, 302, 820)$ GeV. We see that the bosonic modes dominate the \tilde{t}_2 and \tilde{b}_2 decays in a wide range of $M_{\tilde{Q}}$. (Notice that the decay into a gluino is dominant above its threshold.)

For large m_A the decays into H^0 , A^0 , and H^\pm are phase-space suppressed. However, the remaining gauge boson modes can still be dominant. For $M_{\tilde{Q}} = 500$ GeV, $\mu = 1000$ GeV, $A = 1000$ GeV, and $\tan\beta = 3$ we have, for instance, $(m_{\tilde{t}_1}, m_{\tilde{t}_2}, m_{\tilde{b}_1}, m_{\tilde{b}_2}, m_{\tilde{\chi}_1^+}, m_{\tilde{\chi}_1^0}) = (365, 610, 501, 558, 294, 148)$ GeV with $\text{BR}(\tilde{t}_2 \rightarrow \tilde{q}H) = (68, 58, 32, 1)\%$ and $\text{BR}(\tilde{t}_2 \rightarrow \tilde{q}V) = (18, 24, 39, 57)\%$ for $m_A = (110, 200, 240, >250)$ GeV. As for the dependence on the parameter M , our results do not change significantly for smaller values of M , as long as decays into gluino are kinematically forbidden.

Let us now discuss the signatures of the \tilde{t}_2 and \tilde{b}_2 decays. Typical signals of the decays into bosons (Eqs. (2) and (3)) and of those into fermions (Eq. (1)) are shown in Table 1 of Ref. [16]. In principle, the final states of both types of decays can be identical. For example, the final state of the decay chain (a) $\tilde{t}_2 \rightarrow \tilde{t}_1 + (h^0, H^0, A^0 \text{ or } Z^0) \rightarrow (t\tilde{\chi}_1^0) + (b\bar{b}) \rightarrow (bq\bar{q}'\tilde{\chi}_1^0) + (b\bar{b})$ has the same event topology as that of (b) $\tilde{t}_2 \rightarrow t + \tilde{\chi}_{2,3,4}^0 \rightarrow t + ((h^0, H^0, A^0 \text{ or } Z^0) + \tilde{\chi}_1^0) \rightarrow t + (b\bar{b}\tilde{\chi}_1^0) \rightarrow (bq\bar{q}') + (b\bar{b}\tilde{\chi}_1^0)$. Likewise (c) $\tilde{t}_2 \rightarrow \tilde{b}_{1,2} + (H^+ \text{ or } W^+) \rightarrow (b\tilde{\chi}_1^0) + (q\bar{q}')$ has the same event topology as (d) $\tilde{t}_2 \rightarrow b + \tilde{\chi}_{1,2}^+ \rightarrow b + ((H^+ \text{ or } W^+) + \tilde{\chi}_1^0) \rightarrow b + (q\bar{q}'\tilde{\chi}_1^0)$. However, the decay structures and kinematics of the two modes (a) and (b) ((c) and (d)) are quite different from each other, since the $\tilde{\chi}_1^0$ (supposed to be the lightest supersymmetric particle (LSP) and hence a missing particle in case of R-parity conservation) is emitted from \tilde{t}_1 and $\tilde{\chi}_{2,3,4}^0$ ($\tilde{b}_{1,2}$ and $\tilde{\chi}_{1,2}^+$), respectively. This could result in significantly different event distributions (e.g. missing energy-momentum distribution) of the \tilde{q}_2 decays into gauge or Higgs bosons compared to the decays into fermions. Hence the possible dominance of the former decay modes could have an important impact on the search for \tilde{t}_2 and \tilde{b}_2 , and on the measurement of the MSSM parameters. Therefore, the effects of the bosonic decays should be included in the Monte Carlo studies of \tilde{t}_2 and \tilde{b}_2 decays.

In conclusion, we have shown that the \tilde{t}_2 and \tilde{b}_2 decays into Higgs or gauge bosons (such as $\tilde{t}_2 \rightarrow \tilde{t}_1 + (h^0, H^0, A^0 \text{ or } Z^0)$ and $\tilde{t}_2 \rightarrow \tilde{b}_{1,2} + (H^+ \text{ or } W^+)$) can be dominant in a wide range of the MSSM parameter space due to large Yukawa couplings and mixings of \tilde{t} and \tilde{b} . Compared to the conventional fermionic modes (such as $\tilde{t}_2 \rightarrow t + (\tilde{\chi}_i^0 \text{ or } \tilde{g})$ and $\tilde{t}_2 \rightarrow b + \tilde{\chi}_j^+$), these bosonic decay modes can have significantly different decay structures and distributions. This could have an important impact on the searches for \tilde{t}_2 and \tilde{b}_2 and

on the determination of the MSSM parameters at future colliders.

Acknowledgements

The work of A.B., H.E., S.K., W.M., and W.P. was supported by the “Fonds zur Förderung der wissenschaftlichen Forschung” of Austria, project no. P10843-PHY. The work of Y.Y. was supported in part by the Grant-in-aid for Scientific Research from the Ministry of Education, Science, and Culture of Japan, No. 10740106, and by Fuuju-kai Foundation.

References

- [1] See, e.g.:
H. Baer et al., contributed chapter to DPF study group on Electroweak Symmetry Breaking and Beyond the Standard Model, published by APS, DPF (hep-ph/9503479);
A. Bartl et al., Proc. of the 1996 DPF/DPB Summer Study on New Directions for High-Energy Physics, Snowmass, Colorado, 1996, p. 693
- [2] For a review, see:
H. P. Nilles, Phys. Rep. 110 (1984) 1;
H.E. Haber and G.L. Kane, Phys. Rep. 117 (1985) 75;
R. Barbieri, Riv. Nuov. Cim. 11 (1988) 1.
- [3] A. Bartl, W. Majerotto, and W. Porod, Z. Phys. C 64 (1994) 499; C 68 (1995) 518 (E).
- [4] A. Bartl, H. Eberl, S. Kraml, W. Majerotto, W. Porod, and A. Sopczak, Z. Phys. C 76 (1997) 549.
- [5] J. Ellis and S. Rudaz, Phys. Lett. B 128 (1983) 248.
- [6] J. F. Gunion and H. E. Haber, Nucl. Phys. B 272 (1986) 1; B 402 (1993) 567 (E).
- [7] J. Ellis, G. Ridolfi, and F. Zwirner, Phys. Lett. B 262 (1991) 477.
- [8] W. Porod, PhD thesis, Univ. Vienna, 1997 (hep-ph/9804208)
- [9] G. Altarelli, J. Ellis, G. F. Guidice, S. Lola, and M. L. Mangano, Nucl. Phys. B 506 (1997) 3;
J. Ellis, S. Lola, and K. Sridhar, Phys. Lett. B 408 (1997) 252.
- [10] M. Drees and K. Hagiwara, Phys. Rev. D 42 (1990) 1709.

- [11] J. P. Derendinger and C. A. Savoy, Nucl. Phys. B 237 (1984) 307.
- [12] ALEPH Collab., R. Barate et al., CERN-PPE/97-128;
 DELPHI Collab., P. Abreu et al., Eur. Phys. J. C 1 (1998) 1;
 L3 Collab., M. Acciarri et al., CERN-PPE/97-130 (to appear in Eur. Phys. J. C);
 OPAL Collab., K. Ackerstaff et al., Eur. Phys. J. C 2 (1998) 213.
- [13] OPAL Collab., K. Ackerstaff et al., Z. Phys. C 75 (1997) 409;
 ALEPH Collab., R. Barate et al., Phys. Lett. B 413 (1997) 431.
- [14] ALEPH Collab., R. Barate et al., Phys. Lett. B 412 (1997) 173;
 DELPHI Collab., P. Abreu et al., Eur. Phys. J. C 2 (1998) 1;
 A. Sopczak, Talk at the 1st Int. Workshop on Non-Accelerator Physics, Dubna, July 1997, to be published in the proceedings (hep-ph/9712283).
- [15] DØ Collab., S. Abachi et al., Phys. Rev. Lett. 75 (1995) 618; Phys. Rev. Lett 76 (1996) 2222;
 CDF Collab., F. Abe et al., Phys. Rev. D 56 (1997) 1357.
- [16] A. Bartl, K. Hidaka, Y. Kizukuri, T. Kon, and W. Majerotto, Phys. Lett. B 315 (1993) 360;
 A. Bartl, H. Eberl, K. Hidaka, T. Kon, W. Majerotto, and Y. Yamada, Phys. Lett. B 389 (1996) 538.

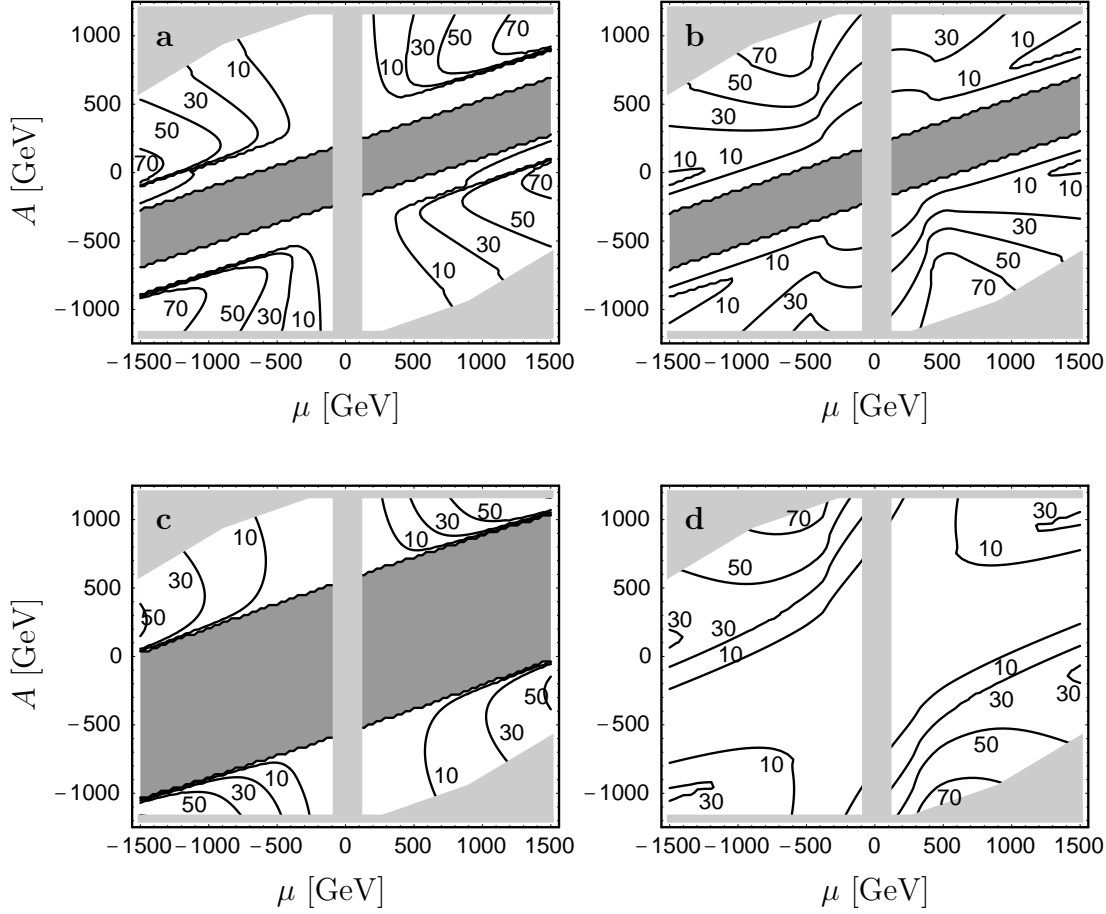


Figure 1: Branching ratios (in %) of \tilde{t}_2 and \tilde{b}_2 decays in the μ - A plane for $A_t = A_b \equiv A$, $M_{\tilde{Q}} = 500$ GeV, $M_{\tilde{U}} = 444$ GeV, $M_{\tilde{D}} = 556$ GeV, $M = 300$ GeV, $m_A = 150$ GeV, and $\tan \beta = 3$. (a) $\sum \text{BR}[\tilde{t}_2 \rightarrow \tilde{t}_1 + (h^0, H^0, A^0), \tilde{b}_{1,2} + H^+]$, (b) $\sum \text{BR}[\tilde{t}_2 \rightarrow \tilde{t}_1 + Z^0, \tilde{b}_{1,2} + W^+]$, (c) $\text{BR}[\tilde{b}_2 \rightarrow \tilde{t}_1 + H^-]$, (d) $\text{BR}[\tilde{b}_2 \rightarrow \tilde{t}_1 + W^-]$. In the dark grey areas the decays are kinematically not allowed; the light grey areas are excluded by the conditions (i) to (vi) given in the text.

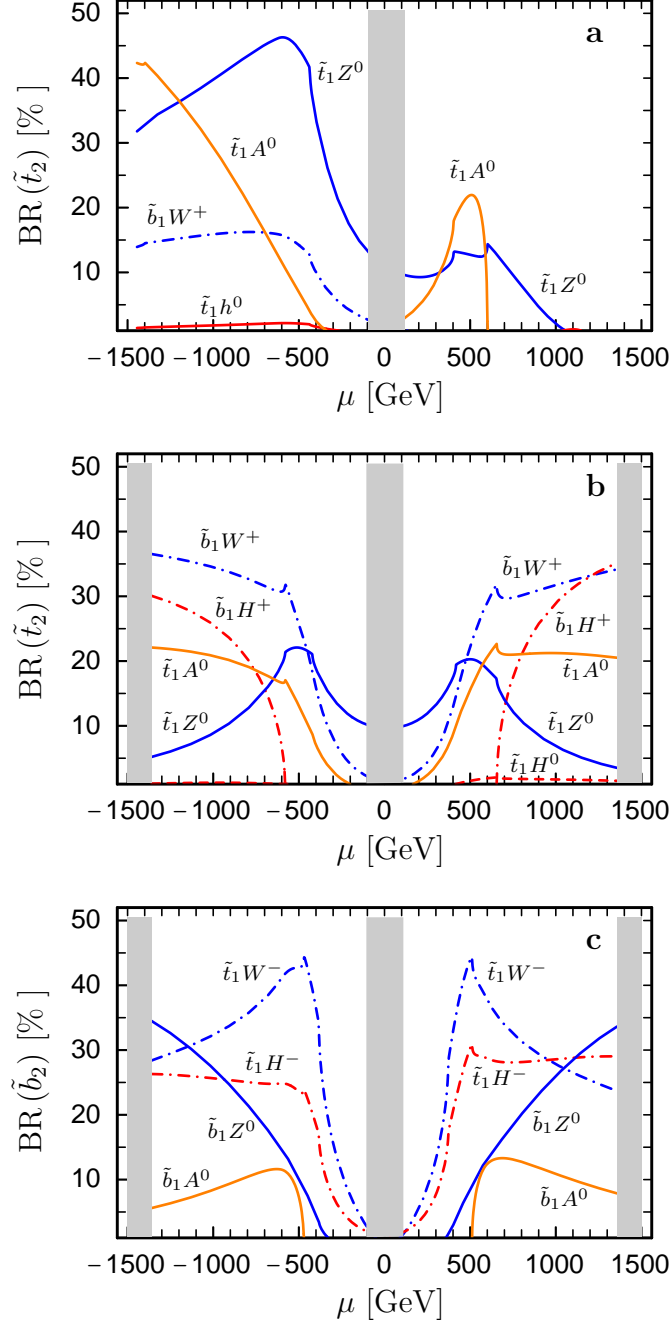


Figure 2: μ dependence of \tilde{t}_2 and \tilde{b}_2 decay branching ratios for $M_{\tilde{Q}} = 500$ GeV, $M_{\tilde{U}} = 444$ GeV, $M_{\tilde{D}} = 556$ GeV, $A_t = A_b = 600$ GeV, $M = 300$ GeV, $m_A = 150$ GeV, (a) $\tan\beta = 3$, (b) and (c) $\tan\beta = 30$. The grey areas are excluded by the conditions (i) to (vi) given in the text.

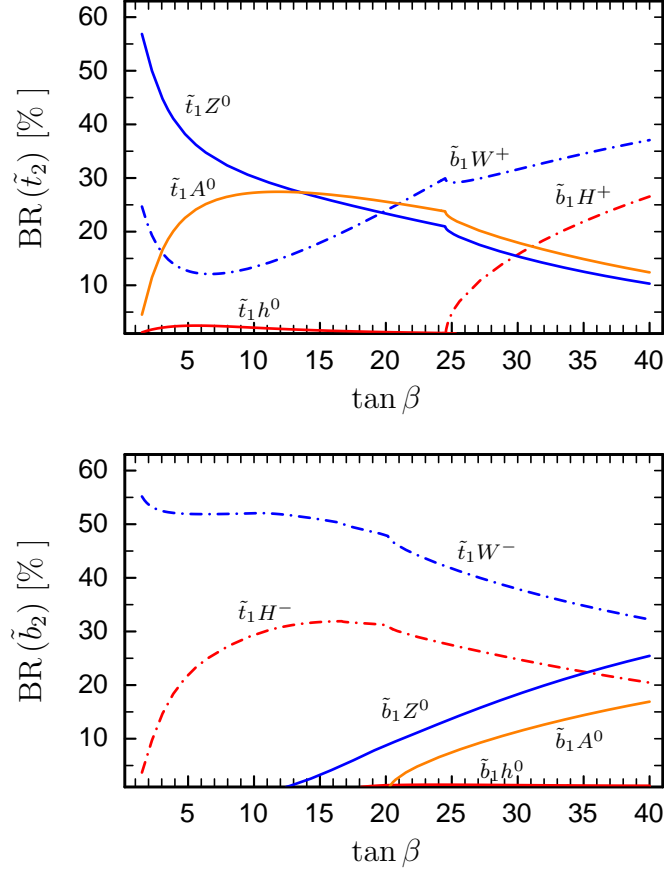


Figure 3: $\tan \beta$ dependence of \tilde{t}_2 and \tilde{b}_2 decay branching ratios for $M_{\tilde{Q}} = 500$ GeV, $M_{\tilde{U}} = 444$ GeV, $M_{\tilde{D}} = 556$ GeV, $A_t = A_b = 600$ GeV, $\mu = -700$ GeV, $M = 300$ GeV, and $m_A = 150$ GeV.

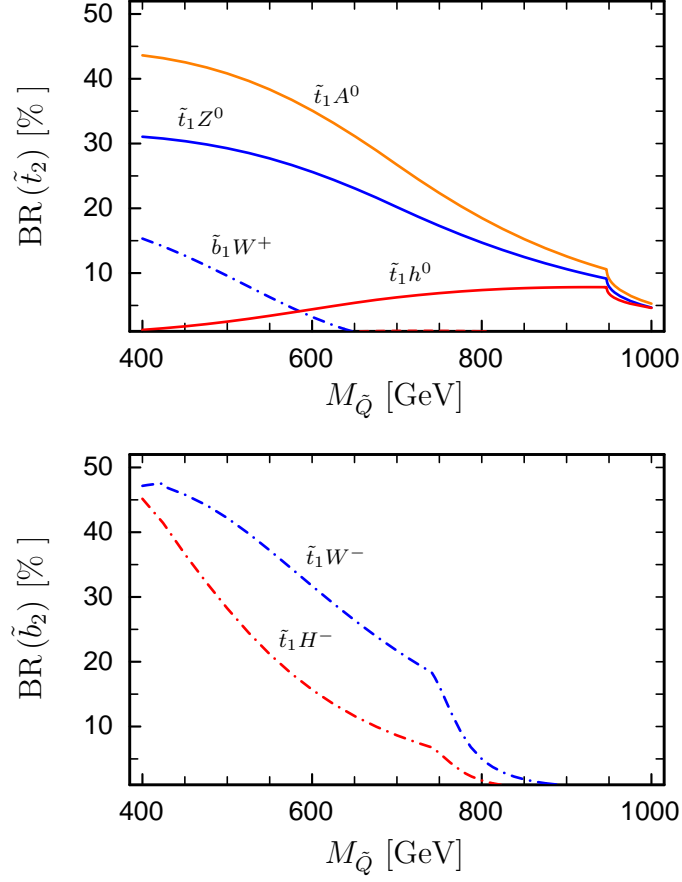


Figure 4: $M_{\tilde{Q}}$ dependence of \tilde{t}_2 and \tilde{b}_2 decay branching ratios for $M_{\tilde{U}} = \frac{8}{9} M_{\tilde{Q}}$, $M_{\tilde{D}} = \frac{10}{9} M_{\tilde{Q}}$, $A_t = A_b = 400 \text{ GeV}$, $\mu = -1000 \text{ GeV}$, $M = 300 \text{ GeV}$, $m_A = 150 \text{ GeV}$, and $\tan \beta = 3$.